

CHAPTER 73

A Numerical Investigation of The Longshore Current Profile for Multiple Bar/Trough Beaches

Steven K. Baum¹ and David R. Basco²

Abstract

A numerical model is developed which calculates the longshore current profile for an arbitrary bottom profile. The basis of the model is the use of radiation stress theory in a longshore momentum balance equation which includes a driving stress, a bottom stress, and a lateral mixing stress. Each of the stresses is derived from previously developed formulations, rederiving them to take into account separate cross shore variations in the wave height and the water depth, as well as the wave approach angle. This is done to dispense with the constant wave breaking index assumption used to model wave decay in the surf zone, which is rejected as unrealistic for natural beaches. A numerical model is used to calculate distributions of the wave height and water depth across the surf zone for arbitrary, yet realistic, bottom profiles. A numerical model of the theoretically derived longshore momentum balance equation is developed and solved using the distributions obtained from the wave decay model. The profiles calculated are compared to previous theoretical models and to laboratory and field measurements.

1.0 Introduction

All present-day longshore current models are based on concepts of radiation stress as first introduced by Longuet-Higgins and Stewart (1964). Longuet-Higgins (1970) and others applied these time-averaging principles to the depth-integrated momentum balance equation to obtain the longshore current profile. The component stresses (radiation shear stress, bottom stress and lateral turbulent mixing stress) in the alongshore momentum equation are expressed in terms of three key variables to obtain the current profile as a function of distance from the shoreline. These three variables are the mean water depth, the wave height and the wave angle. More accurately, the gradient of the longshore current across the surf zone is computed using the gradients of water depth, wave height and wave angle across the surf zone.

The original model of Longuet-Higgins (1970) employed many simplifying assumptions regarding these three variables. This permitted an analytical solution to be obtained which facilitated

¹Ph.D. Candidate, Department of Oceanography, Texas A&M University, College Station, TX

²Professor and Director, Coastal Engineering Institute, Department of Civil Engineering, Old Dominion University, Norfolk, VA 23508

physical understanding. For example, Longuet-Higgins (1970) related the wave height to the water depth using a constant wave breaking index model. He also assumed a small incident wave angle and neglected the wave-induced set-up (set-down) effects on the mean water depth which became the sole variable of interest.

Subsequent investigators have relaxed or eliminated many of these assumptions. However, all investigators to date have continued to use the wave breaking index simplification which requires specification of either a linear or monotonically decreasing bathymetric profile. Most natural beaches have single or multiple bar-trough features at sometime during yearly cycles. Multiple wave breaking and reforming regions across these surf zones produce a complex wave height distribution that is clearly not amenable to the use of the wave breaking index to specify the wave height as directly proportional to the water depth.

A mathematical model has been developed that makes no simplifying assumptions regarding the three above mentioned key variables. Water depth, wave height and wave angle can vary separately across the surf zone. Section 2 presents all the theoretical details including the wave height decay (and recovery) model for use across arbitrary, realistic bottom profiles. Because an analytic solution is not possible for realistic bathymetry, Section 3 discusses the computer algorithm based on a finite-difference analog of the governing ordinary differential equation and the solution method. All test results are summarized in Section 4 including those for an artificially devised beach profile with three wave breaking-reforming regions and one final breaker zone on the exposed beach face.

The results are for depth-averaged, longshore current profiles induced by uniform breaking waves on infinite beaches of arbitrary cross-sectional shape. A complete report of this entire study is available (Baum, 1985).

2.0 Theoretical Development

Consider the depth-integrated and time-averaged horizontal momentum balance equation for steady, uniform motion as depicted schematically in Figure 1.

$$\text{Cross-shore}(x) \quad \frac{dS_{xx}}{dx} + \rho g h \frac{d\bar{\eta}}{dx} = 0 \quad (1)$$

$$\text{Alongshore}(y) \quad \frac{dS_{xy}}{dx} - \bar{\tau}_B + \frac{dT_L}{dx} = 0 \quad (2)$$

where: S_{xx} = the shorenormal radiation stress component;
 S_{xy} = the shear radiation stress component;
 $\bar{\eta}$ = the mean water level set-up (set-down);
 $\bar{\tau}_B$ = the time-averaged bottom shear stress;
 T_L = the lateral, turbulent mixing stress;

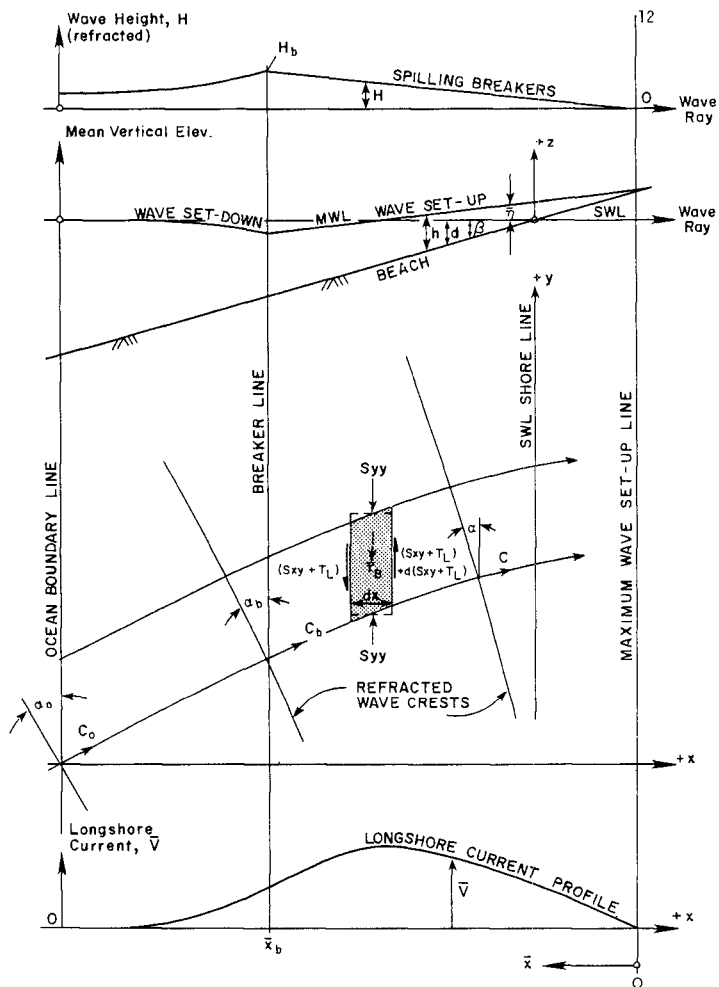


Figure 1. Schematic of surf zone (from Basco, 1982)

ρ = the water mass density; and
 g = the acceleration due to gravity.

Equations (1) and (2) are decoupled in the sense that feedback effects of the currents on the wave heights are normally neglected. The cross-shore equation (1) is solved for the wave set-up as part of the method for obtaining the wave height and mean water depth as described below. Equation (2) is then solved for the longshore current profile using the results from (1) and the expressions for the stresses also described below. The complete, unsteady flow, two-dimensional forms of these equations can be found in Basco (1982).

2.1 Wave Energy Decay and Reforming Model

A model is needed to shoal a wave to the breaking point and then calculate the wave energy decay to a point of wave reformation where wave shoaling begins anew to a new break point or the shoreline. For this purpose the newly developed model of Dally et al. (1984) was employed.

The physical idea behind this model is that after a wave breaks it dissipates energy continuously until some stable wave height is reached where breaking stops and wave reforming and shoaling begins. The key assumption in this empirical approach is that the energy dissipation during breaking is proportional to difference between the actual and stable wave energy flux at any point. Using the definition of wave energy density and after integration this gives

$$(H^2 - H_s^2)_2 = (H^2 - H_s^2)_1 \exp\left(\frac{K}{d} \Delta x\right) \quad (3)$$

where: H_s = the stable wave height
 d = the still water depth
 Δx = the distance step between points (1) and (2) where evaluation of the new wave height, H takes place, and
 K = a wave energy decay factor.

A laboratory investigation conducted by Dally et al. (1984) to calibrate the model obtained best values for K of 0.17 and for H_s to be $0.4h$. These coefficients we employed in the present model. Equation (3) reveals this to be an exponential wave energy decay model.

2.2 Cross-Shore Momentum Balance

Using the classical, linear wave theory definition for S_{xx} and wave energy density, E , Equation (1) when rearranged becomes

$$\frac{d\bar{\eta}}{dx} = \frac{2 + \cos 2\theta}{16h} \frac{d(H^2)}{dx} \quad (4)$$

to relate the mean water level set-up to the wave height. The wave

angle distribution across the surf zone was obtained from classic refraction methods using Snell's law.

An iterative procedure was followed in that first Equation (3) using the still water depth was employed to estimate the $H(x)$ distribution. From (4) this gave $\bar{\eta}(x)$ from which a second iteration using $h=d+\bar{\eta}$ in (3) produced convergence to an acceptable tolerance after only 2-3 iterations. At this point, distributions of mean water depth, $h(x)$, wave height, $H(x)$ and wave angle, $\theta(x)$ are completely specified across the surf zone.

2.3 Longshore Momentum Balance

Equation (2) expresses a balance between the driving stress gradient, bottom stress and lateral (turbulent) mixing stress gradient. Previous formulations judged best in each case have been rederived to take into account separate variations of h , H and θ across the surf zone.

Driving Stress. Using classical, linear, shallow water wave theory, the shear radiation stress component can be shown to be (Longuet-Higgins, 1970)

$$S_{xy} = \frac{1}{8} \rho g^{3/2} \left(\frac{\sin \theta}{c} \right) H^2 h^{1/2} \cos \theta \tag{5}$$

where we now also have c , the wave celerity. Using chain rule differentiation the driving stress gradient becomes

$$\frac{dS_{xy}}{dx} = \frac{1}{8} \rho g^{3/2} \left(\frac{\sin \theta}{c} \right) \left\{ h^{1/2} \cos \theta \frac{\partial H^2}{\partial x} + H^2 \cos \theta \frac{\partial h^{1/2}}{\partial x} + H^2 h^{1/2} \frac{\partial \cos \theta}{\partial x} \right\} \tag{6}$$

Bottom Stress. We adopt a bottom stress formulation for large wave approach angles as originally formulated by Liu and Dalrymple (1978) and modified to accommodate separate variations of h and H . The expression employed is

$$\bar{\tau}_B = \frac{\rho f g^{1/2} H (1 + \sin^2 \theta)}{8 \pi h^{1/2}} v \tag{7}$$

where: f = a dimensionless friction coefficient, and
 v = the time-averaged, depth-integrated longshore current.

Lateral Mixing Stress. We adopt a lateral mixing stress formulation using a classical, eddy viscosity approach. Following Battjes (1975), we take the water depth as reference length scale and reference velocity related to the local energy dissipation rate, D , where

$$D = \frac{\partial}{\partial x} \left[\frac{1}{8} \rho g^{3/2} H^2 h^{1/2} \cos \theta \right] \tag{8}$$

Again using chain rule differentiation (8) yields

$$D = \frac{1}{8} \rho g^{3/2} G(x) \quad (9)$$

where

$$G(x) = \left\{ h^{1/2} \cos \theta \frac{\partial H^2}{\partial x} + H^2 \cos \theta \frac{\partial h^{1/2}}{\partial x} + H^2 h^{1/2} \frac{\partial \cos \theta}{\partial x} \right\} \quad (10)$$

From the basic relationship

$$\tau_L = \rho \epsilon h \frac{dv}{dx} = \rho \left(M h \left(\frac{D}{\rho} \right)^{1/3} \right) h \frac{dv}{dx} \quad (11)$$

where: ϵ = the turbulent eddy viscosity, and
 M = a turbulent closure coefficient

the gradient of the mixing stress becomes

$$\frac{\partial \tau_L}{\partial x} = M \rho \left(\frac{1}{8} g^{3/2} \right)^{1/3} \left\{ \frac{\partial h^2}{\partial x} G(x)^{1/3} \frac{dv}{dx} + h^2 \frac{\partial [G(x)^{1/3}]}{\partial x} \frac{dv}{dx} + h^2 G(x)^{1/3} \frac{d^2 v}{dx^2} \right\} \quad (12)$$

2.4 Longshore Current Profile Equation

Combining equations (2), (6), (7) and (12) gives $\frac{d^2 v}{dx^2}$ with $G(x)$ given by (10)

$$\frac{d^2 v}{dx^2} + \left[\frac{\beta_1(x)}{\beta_2(x)} \right] \frac{dv}{dx} - \left[\frac{B \beta_2(x)}{A \beta_2(x)} \right] v + \left[\frac{C G(x)}{A \beta_2(x)} \right] = 0 \quad (13)$$

where:

$$\beta_1(x) = \frac{\partial h^2}{\partial x} G(x)^{1/3} + h^2 \frac{\partial G(x)^{1/3}}{\partial x} \quad (a)$$

$$\beta_2(x) = h^2 G(x)^{1/3} \quad (b)$$

$$\beta_3(x) = \frac{H [1 + \sin^2 \theta]}{h^{1/2}} \quad (c) \quad (14)$$

$$A = \frac{1}{2} \rho g^{1/2} M \quad (d)$$

$$B = \frac{1}{8} \frac{\rho f g^{1/2}}{\pi} \quad (e)$$

$$C = \frac{1}{8} \rho g^{3/2} \left(\frac{\sin \theta}{c} \right) \quad (f)$$

Equation (13) is a nonhomogeneous, ordinary, second-order differential equation inside the breaker line. It becomes homogenous outside the breaker line because the group of coefficients given by $CG(x)$ is zero there.

The boundary conditions are identical to those employed by Longuet-Higgins (1970) in the original theory. This means taking zero velocity at the new (set-up) shoreline, matching both velocity and its gradient at the breaker line for inner and outer solutions and letting the velocity approach zero far outside the breaker line.

3.0 Numerical Solution

Equation (13) can be written

$$\frac{d^2V}{dx^2} + C_1 \frac{dV}{dx} - C_2 V + C_3 = 0 \quad (15)$$

and must be solved numerically because the coefficients, C_1 , C_2 and C_3 are nonconstant in x . The numerical method employed falls in a general class called "shooting" methods whereby the slope at a known value of the dependent variable ($v=0$ at $x=0$) is first assumed thereby creating an initial value problem which is solved by the fourth-order, Runge-Kutta method. This procedure is repeated until the calculated value at the second boundary point is within a specified tolerance of the actual function value at this location. An estimate of the initial slope was made using the original, analytical solution of Longuet-Higgins (1970) from which two bracketing guesses permit a linear interpolation to accelerate convergence. Because of the two internal, boundary conditions at the breaker line, the numerical algorithm adopted utilized two "shooting" methods, one for the region inside and a second for the zone outside the breaker line. For practical reasons, a distance of approximately three surf zone widths proved reasonable for the limit of the outer region where the current velocity returned to nearly zero values.

4.0 Test Results

4.1 Basic Tests

A series of basic tests were initially conducted to compare numerical model results with those previously published for simple cases using a constant wave breaker index.

Plane Beach. An initial comparison was made to the original analytical results of Longuet-Higgins (1970) for a plane beach. This required making the same simplifying assumptions (constant breaker index, neglect of wave set-up and refraction effects) and conversion of the bottom friction and lateral mixing coefficients to those employed by Longuet-Higgins. In the original model, the mixing parameter, P is defined as

$$P = \frac{N \pi \tan \beta}{C_f Y} \quad (16)$$

where: $\tan \beta = m$, the beach slope;
 $c_f = \frac{1}{2}f$, the bottom friction coefficient;
 $N = M \left(\frac{2}{10} \right)^{1/3} \gamma (\tan \beta)^{1/3}$, the lateral mixing coefficient
and $\gamma = \frac{H}{h}$, the wave breaking index.

The curves for both the analytical model of Longuet-Higgins (1970) and the present numerical model for identical data sets are shown in Figure 2. The chosen data results in $P = 0.106$ for this case. Both curves are identical in shape and size inside the breaker line (dimensionless distance of unity) but slightly different outside. The difference in the results outside the breaker line is simply due to different wave transformation models being used to shoal the wave so that equivalence is theoretically not possible. In Figure 2 and subsequent plots, all velocities are normalized by the breaker line, longshore current with no mixing as first used by Longuet-Higgins (1970).

Large Wave Angle. The model of Liu and Dalrymple (1978) included wave set-up and refraction effects on the velocity profile because their main intent was to study the effects of large incident wave angles. Consequently, they neglected lateral mixing but revised the bottom friction stress formulation to account for strong longshore currents. Figure 3 presents numerical model results from this study ($P=0.106$) and reveals a decrease in velocity with increasing wave angle, as expected. No comparison with the published results of Liu and Dalrymple (1978) was possible since it was learned that their values are incorrect by some factor (Vemulakonda, 1986). However, both models for very small incidence angle gave nearly identical results compared to the reference velocity profile (triangular with no mixing) of Longuet-Higgins (1970).

Wave Decay Model. A final base test compared differences due to the specification of the wave decay model. A plane beach, small wave angle and no set-up test was devised with $P=0.10$ but using a slightly different combination of variables. These specifications assured that the differences in the velocity profile were due only to differences to the wave height field.

Using identical data sets, the current profiles from both the numerical model and the original, analytical model of Longuet-Higgins (1970) are shown in Figure 4. Considerable differences now exist. These can be explained from the fact that the wave height decreases linearly in the analytical model and exponentially in the numerical model. In general, the wave decay model of Dally et al. (1984) flattens the profile inside and steepens it outside the breaker line on a plane beach.

4.2 Laboratory Tests

The present numerical model has been compared to laboratory measurements by Mizuguchi et al. (1978, Case 3) as shown in Figure 5. Coefficients for friction and lateral turbulent mixing as determined to give a "best fit" at the maximum velocity by Kraus and

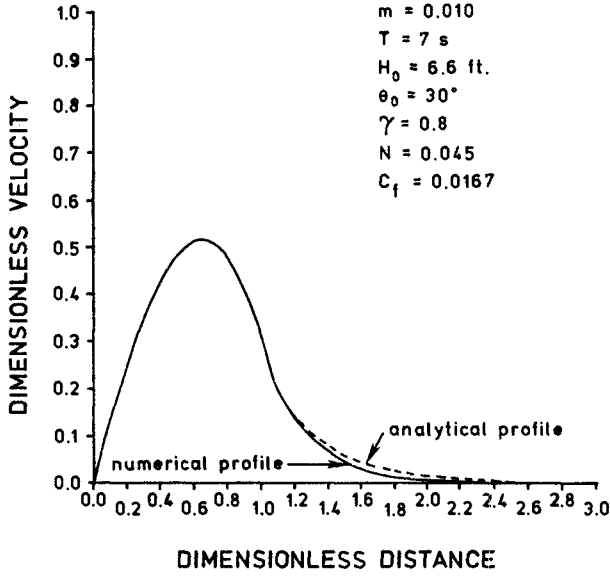


Figure 2. Comparison of numerical model to analytical solution of Longuet-Higgins for identical parameters

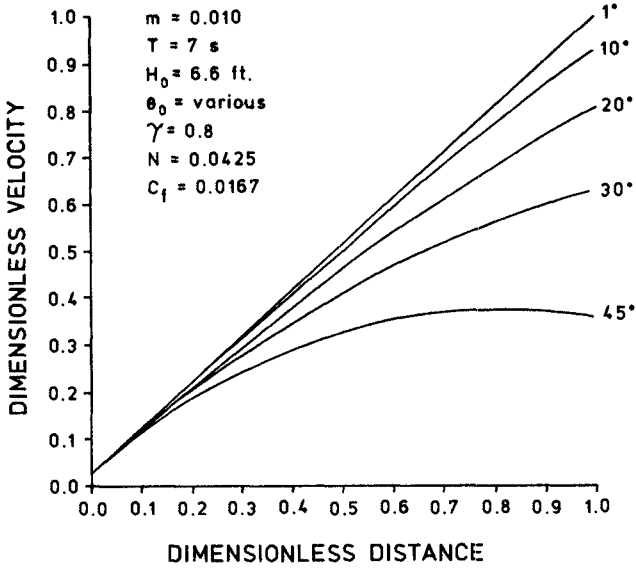


Figure 3. Numerical model results for large angle effects without lateral mixing

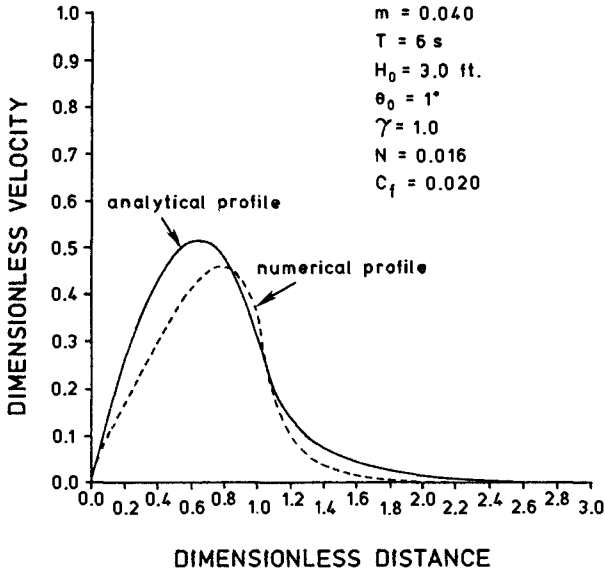


Figure 4. Comparison of differences in velocity profiles due to wave decay specification

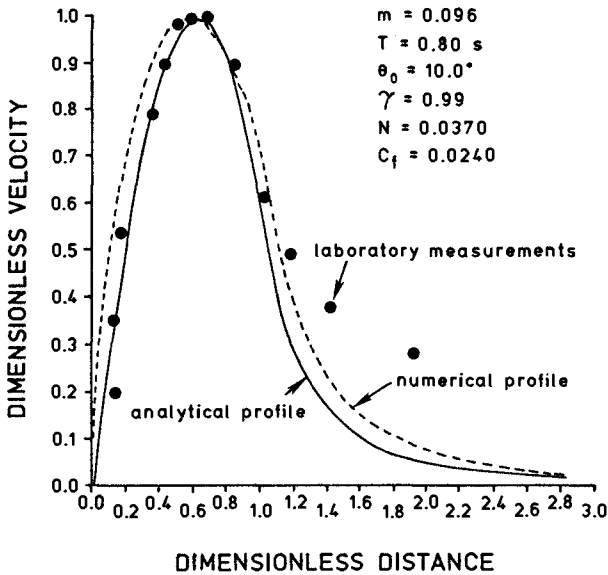


Figure 5. Comparison of predicted velocity profile with laboratory measurements of Mizuguchi et al. (1978 Case 3)

Sasaki (1979) for their model were employed. The analytical solution of Longuet-Higgins (1970) is also shown ($P=0.47$). The results of the Kraus and Sasaki (1979) model fall somewhere between those shown on Figure 5 and all three give good agreement with measured values inside the breaker line.

The discrepancies outside are primarily due to laboratory-scale effects as discussed by Basco (1982), Battjes (1978) and Kraus and Sasaki (1979) in their use of this data set to test their model. Additional laboratory-scale data sets are now available for plane beaches to test numerical models (e.g. Visser, 1984). No laboratory data is available for a bar-trough beach profile.

4.3 Field Tests

Field measurements of wave-induced longshore currents under uniform and steady wave conditions are difficult to obtain. Because of continuously varying field conditions including local winds not modeled and scales of velocity traces recorded by modern instruments, a standard, universally accepted averaging time to define the longshore current has yet to be determined. We show one comparison here of the numerical model with the field measurements performed by Kraus and Sasaki (1979) in a surf zone with two observed wave breaking lines. Their measured velocity and bottom profiles are displayed in Figure 6. Figure 7 displays the numerically predicted longshore profile using bottom friction and lateral mixing parameters as specified by these same investigators (Kraus and Sasaki, 1979) for use in their model. Both numerical and field plots show a secondary velocity maximum near the shoreline. It is evident that a "best fit" profile could be obtained for the present model by appropriate manipulation of the friction and mixing parameters to values different than those suggested by Kraus and Sasaki (1979) for their model. This has not been done since the objective was simply to simulate a multiple-peaked, longshore current profile.

4.4 Multiple Bar-Trough Beaches

In the absence of a laboratory data-set under controlled conditions for a bar-trough beach profile with multiple breaker and reforming regions, no definitive answer is yet possible as to the adequacy of the present numerical model. Never-the-less, an artificial yet realistic profile was constructed with three offshore bars as depicted in Figure 8. The average slope is 0.048. This profile is typical of those found on lower energy, Gulf of Mexico beaches. Waves broke over the three bars and within the inner slope to give four breaker lines and theoretically, four peaks in the longshore current profile.

The current profile predicted by the numerical model for the contrived bathymetry and representative parameters is shown in Figure 9. Also shown is the analytical model profile of Longuet-Higgins (1970) for an average slope of the entire profile. The profile of the multiple breaker case is seen to be similar overall to the profile developed from the analytical solution for a constant slope.

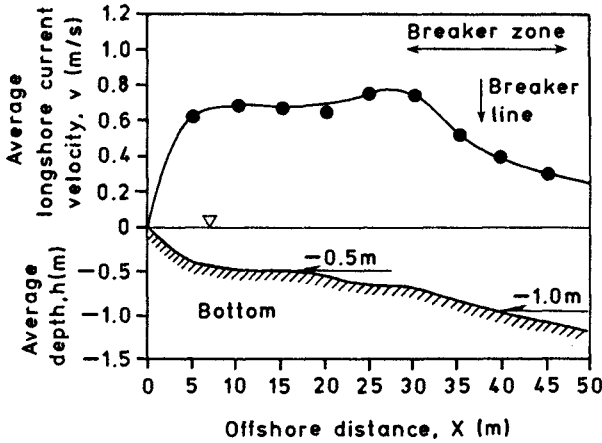


Figure 6. Measured velocity and depth profiles for two breaker Line situation in field (from Kraus and Sasaki, 1979)

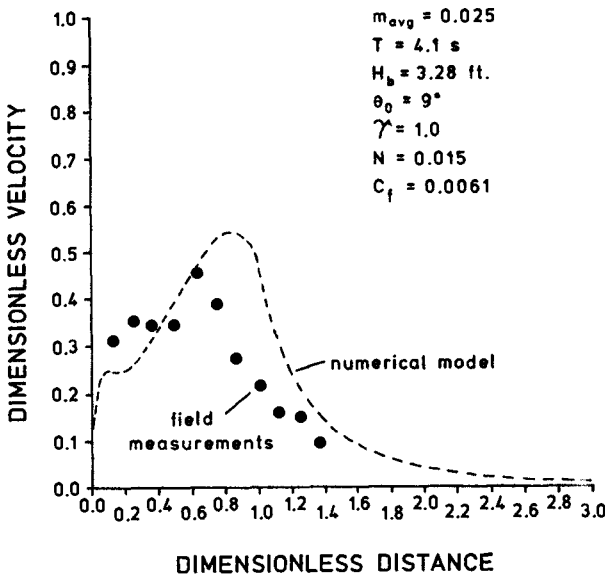


Figure 7. Comparison of predicted velocity profile to measured field profile for two breaker line case.

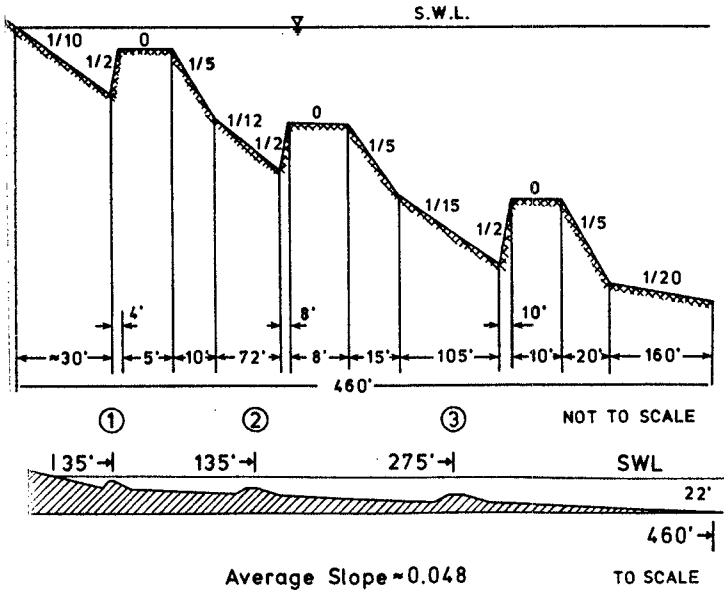


Figure 8. Artificial bottom profile to induce multiple wave breaking

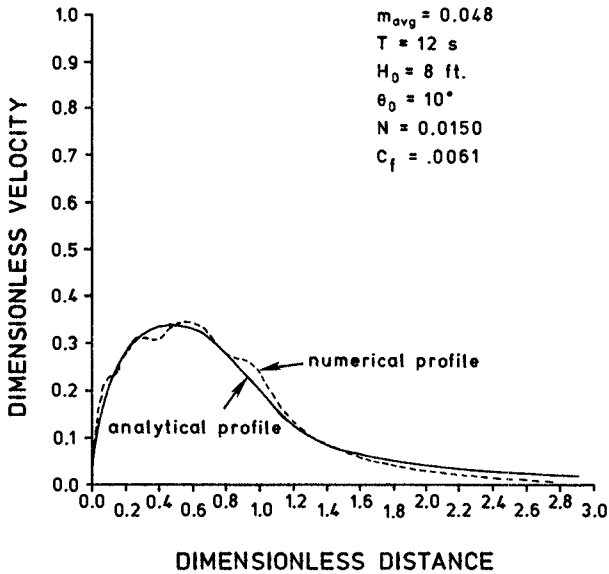


Figure 9. Comparison of velocity profiles due to artificial bathymetry.

The difference is simply four smaller humps present in the overall profile developed by the present model.

The scale of these perturbations is relatively small and similar to the scatter found in field measurements. No attempt was made to make more runs with fewer yet larger bars in lieu of the fact that no laboratory data exists to check the results.

5.0 Summary

A longshore current model for realistic, multiple bar-trough beach profiles has been developed. It permits wave breaking and reforming and this feature in turn produces multiple peaked profiles of the current distribution as found across natural beaches. The model reduces to closed form, analytical solutions for plane beaches. And, it incorporates those components for the stresses that remove the simplifying assumptions made by Longuet-Higgins (1970) in his original model.

It is recommended that more realistic driving stress terms be investigated using radiation stress components derived from nonlinear wave theory outside and broken wave theory inside the surf zone. Svendsen (1984) has shown that the presence of a surface roller in broken surf zone waves increases the radiation stress by 50-100% over that found from linear wave theory. Although limited in scope due to neglect of feedback of currents on the wave field, wind stresses and other natural phenomena, the model is helpful in the development of more general two-dimensional, horizontal models.

References

- Basco, D.R., 1982. Surf Zone Currents, Misc. Rept. No. 82-7. US Army, Corps of Engrs., Coastal Engineering Research Center, Vicksburg, MS, Sept. (in two volumes).
- Battjes, J.A., 1975. Modeling of Turbulence in the Surf Zone, Proceedings; Symposium of Modeling Techniques, Miami, Florida, Vol. 2, pp.1050-1061.
- Battjes, J.A., 1978. A Critical Review of Conventional Models for Some Surf Zone Phenomena; Euromech 102 (Breaking Waves: Surf and Run-Up on Beaches), Univ. of Bristol, Bristol, England, July.
- Baum, S.K., 1985. A Numerical Investigation of the Longshore Current Profile, M.S. Thesis, Ocean Engineering, Texas A&M University, College Station, TX, May.
- Dally, W.R., Dean, R.G., and Dalrymple, R.A., 1984. Modeling Wave Transformation in the Surf Zone, Misc. Paper CERC-84-8, US Army, Corps of Engrs., Coastal Engineering Research Center, Vicksburg, MS.

- Kraus, N.C. and Sasaki, T.O., 1979. Influence of Wave Angle on the Longshore Current, Marine Science Comm., Vol. 5, No. 2, Feb., pp. 91-126.
- Liu, P.L.-F., and Dalrymple, R., 1978. Bottom Frictional Stresses and Longshore Currents Due to Waves With Large Angles of Incidence, J. of Marine Research, Vol. 36, No. 2, May, pp. 357-375.
- Longuet-Higgins, M.S., 1970. Longshore Currents Generated By Obliquely Incident Sea Waves, Parts 1 and 2, J. Geophys. Res., Vol. 75, pp. 6778-6801.
- Longuet-Higgins, M.S., and Stewart, R.W., 1964. Radiation Stress in Water Waves, A Physical Discussion With Applications, Deep-Sea Research, Vol. 11, No. 4, August, pp. 529-562.
- Mizuguchi, M., Oshina, Y. and Horikawa, K., 1978. Laboratory Experiments on Longshore Currents, 25th Coastal Engineering Conference of Japan.
- Svendsen, I.A., 1984. Wave Heights and Set-up in a Surf Zone, Coastal Engineering, Vol. 8, pp. 303-329.
- Vemulakonda, R., 1986, personal communication.
- Visser, P.J., 1984. Uniform Longshore Current Measurements and Calculations, Proceedings, 19th Coastal Engineering Conference, Vol. III, pp. 2192-2207.